
SurgBench: A Unified Large-Scale Benchmark for Surgical Video Analysis

Jianhui Wei^{1,4,*} Zikai Xiao^{1,4,*} Danyu Sun¹ Luqi Gong²
Zongxin Yang³ Zuozhu Liu^{1,4,†} Jian Wu^{1,4,†}

¹Zhejiang University ²Zhejiang Lab ³Harvard University

⁴Zhejiang Key Laboratory of Medical Imaging Artificial Intelligence

*jianhui1.24@intl.zju.edu.cn †zuozhuliu@intl.zju.edu.cn

Abstract

Surgical video understanding is pivotal for enabling automated intraoperative decision-making, skill assessment, and postoperative quality improvement. However, progress in developing surgical video foundation models (FMs) remains hindered by the scarcity of large-scale, diverse datasets for pretraining and systematic evaluation. In this paper, we introduce **SurgBench**, a unified surgical video benchmarking framework comprising a pretraining dataset, **SurgBench-P**, and an evaluation benchmark, **SurgBench-E**. SurgBench offers extensive coverage of diverse surgical scenarios, with SurgBench-P encompassing 53 million frames across 22 surgical procedures and 11 specialties, and SurgBench-E providing robust evaluation across six categories (phase classification, camera motion, tool recognition, disease diagnosis, action classification, and organ detection) spanning 72 fine-grained tasks. Extensive experiments reveal that existing video FMs struggle to generalize across varied surgical video analysis tasks, whereas pretraining on SurgBench-P yields substantial performance improvements and superior cross-domain generalization to unseen procedures and modalities. Our dataset and code are available upon request.

1 Introduction

Surgical video analysis is rapidly becoming a cornerstone for advancing modern surgical care, offering a window into the intricacies of operative procedures (Green et al., 2019). The ability to systematically interpret these videos can significantly impact intraoperative decision-making, automate surgical skill evaluation, and inform postoperative quality improvement initiatives (Loftus et al., 2020; Prebay et al., 2019; Grenda et al., 2016; Levin et al., 2019; Grüter et al., 2023; Dimick and Varban, 2015).

In response to the clinical opportunities, video foundation models (VFMs) have emerged as a powerful framework for surgical video analysis. By leveraging large-scale, diverse datasets, VFMs enable efficient and accurate video modeling, enhancing the potential for surgical video analysis and improving surgical practice Wang et al. (2024); Zhao et al. (2024); Li et al. (2023); Madan et al. (2024). VFMs have demonstrated success in a variety of downstream tasks, benefiting from pre-training on massive datasets that span millions of video clips and several terabytes of data (Wang et al., 2024; Zhang et al., 2025; Tong et al., 2022; Wang et al., 2023a). These datasets encompass diverse video categories, such as YouTube videos, movie trailers, and surveillance footage, enabling models to develop generalizable representations across domains (Li et al., 2023; Madan et al., 2024).

*Co-first author.

†Co-corresponding author.

Datasets	Pretraining Data			Evaluation Data
	# Surgical specialties	# Surgical procedures	# Frames	
Endo-FM (Wang et al. (2023b))	3	3	5M	×
GSViT (Schmidgall et al. (2024))	3	28	70M	×
Surg-3M (Che et al. (2025))	5	35	3M	×
SurgBench (Ours)	11	22	53M	✓ (72 Tasks)

Table 1: Comparison of datasets used for surgical video pretraining and evaluation. Our benchmark achieves advantages in the coverage of surgical specialties and surgical procedures, while also providing comprehensive evaluation standards for downstream tasks.

Despite the proven efficacy of VFMs in general video analysis, their application to surgical video analysis remains in its infancy, primarily due to **the limited diversity of disease types, surgical procedures, and specialties, and insufficient task comprehensiveness in existing pretraining and evaluation datasets**. Disease diversity is constrained, as most datasets focus on specific conditions, such as colorectal cancer (Misawa et al., 2021), limiting model generalization across diverse anatomical variations, comorbidities, and rare diseases (Bar et al., 2020). The coverage in surgical procedures or specialties is narrow, with datasets that predominantly feature specific specialties and minimally invasive procedures, such as laparoscopic cholecystectomy Wang et al. (2022); Twinanda et al. (2016) or robotic prostatectomy Ahmidi et al. (2017), while under-representing open, hybrid, or less standardized surgical techniques. Insufficient task comprehensiveness is apparent in the tendency to emphasize isolated analytical tasks, such as phase classification for a specific procedure (Goodman et al., 2024; Fujii et al., 2024) or instrument recognition (Ma et al., 2021), while neglecting integrated clinical workflows that span multiple temporal and semantic dimensions.

In this paper, we introduce **SurgBench**, a unified, large-scale surgical video benchmarking framework consisting of a pretraining dataset, **SurgBench-P**, and an evaluation benchmark, **SurgBench-E**. The pre-training subset **SurgBench-P** comprises 53 million frames from 16 distinct sources (Figure 1), encompassing 4 primary surgical modalities: laparoscopic, endoscopic, robotic, and open surgery. It spans 22 diverse surgical procedures (e.g., appendectomy, cholecystectomy, colectomy, etc) across 11 medical specialties (see Table 6), directly mitigating procedural and disease-type homogeneities. We further leverage uniform spatiotemporal protocols (e.g., length, frame rate, encoding), aligned with general video understanding benchmarks like Kinetics, across all video sources. This standardization ensures pre-training consistency and supports effective knowledge transfer from general-domain VFMs. Complementing the pre-training corpus, **SurgBench-E** serves as an integrated fine-tuning and hierarchical evaluation framework specifically designed to enrich task diversity and rigorously assess clinical utility. SurgBench-E features 23,004 surgical video clips with granular annotations for 6 distinct surgical understanding task categories, 10 sub-categories, and further delineated into 72 tasks, offering a structured means for comprehensive model evaluation, as detailed in Table 3.

Initial empirical validation underscores the efficacy of this approach: SurgMAE, pre-trained on SurgBench, yields performance gains of 7.9% on downstream tasks relative to models trained on the natural video dataset Kinetics. Our key contributions are as follows:

- We introduce **SurgBench-P**, a large-scale and standardized pretraining dataset (53M frames, 22 procedures, 11 specialties, 4 modalities), designed to address procedural and disease-type homogeneity in surgical video analysis.
- We construct **SurgBench-E**, a comprehensive evaluation benchmark encompassing 72 fine-grained tasks across 6 categories, mitigating task fragmentation and enabling systematic evaluation of clinical utility.
- We validate a self-supervised pretraining pipeline using VideoMAE for superior performance, demonstrating the potential of **SurgBench** to advance research and education in surgery.

2 Related Work

Surgical Video Analysis. Early research in surgical video analytics focused on single diseases or a limited range of tasks, such as surgical phase recognition (Yu et al. (2018)), instrument detection (Yu et al. (2018)), and polyp detection (Ma et al. (2021)). These approaches typically rely on small,

single-center datasets, lacking diversity, which results in task- and scenario-dependent model training with limited generalization capabilities. For instance, studies have been conducted on endoscopic surgeries targeting specific conditions (Nwoye et al. (2022)), laparoscopic hysterectomy procedures (Wang et al. (2022)), colonoscopic videos for polyp detection (Mesejo et al. (2016), Ma et al. (2021)), and capsule endoscopy using PillCAM data (Smetsrud et al. (2021)). Additionally, due to the high cost of annotation, many of these efforts are heavily supervised, making it challenging to scale to a broader range of clinical environments or multi-task learning scenarios.

Surgical Foundation Models. With increasing availability of large-scale surgical video data, researchers have developed Surgical Foundation Models (Wang et al., 2023b; Schmidgall et al., 2024), often leveraging self-supervised learning on diverse datasets for generalizable representations. These models demonstrate superior robustness and cross-domain transferability. More recently, the integration of vision-language and embodied AI approaches (Li et al., 2024; Wang et al., 2025; Li et al., 2025c,a,b; Bi et al., 2024, 2025; Zeng et al., 2024; Guo et al., 2025; Ma et al., 2024; Zhou et al., 2025a,b) has further enhanced semantic understanding and interpretability for complex surgical tasks.

3 Dataset Construction Pipeline

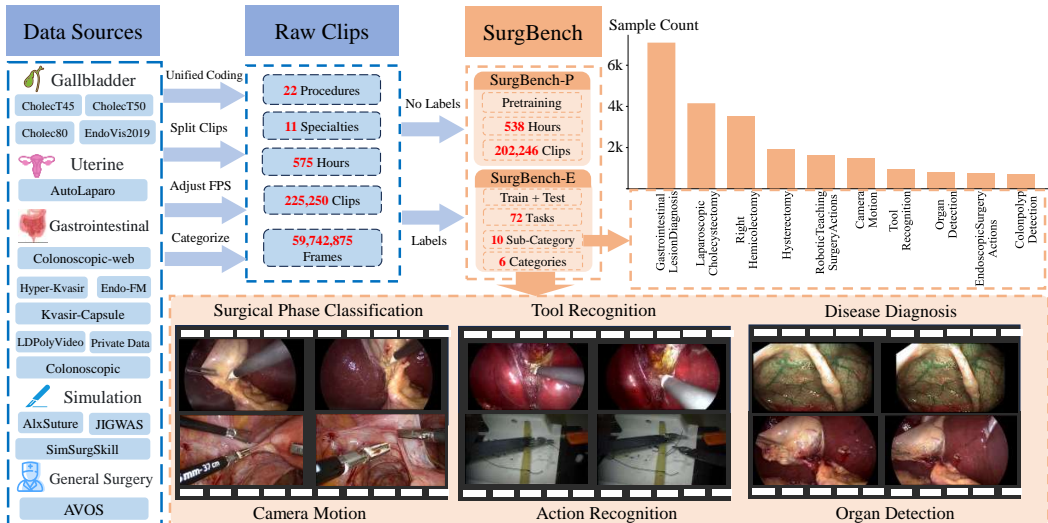


Figure 1: Data construction pipeline of SurgBench. We collect 16 datasets (including private datasets), standardized all video formats to accelerate training, and organized them into SurgBench-P (unlabeled data) and SurgBench-E (labeled data), containing 60 million frames in total. SurgBench-P covers 11 clinical specialties and 22 surgery procedures, while SurgBench-E encompasses 6 categories and 10 sub-categories, totaling 72 tasks. Clip examples are given at the bottom of the figure. The distribution of 10 sub-categories is long-tailed, as shown in the upper right of the figure.

In this section, we introduce the construction pipeline of how we formulate SurgBench, which encompasses SurgBench-P for pretraining models and SurgBench-E for fine-tuning and evaluating models. The whole construction pipeline is shown in Figure 1.

3.1 Dataset Source

We sourced most of the publicly available datasets for surgical video analysis and included 15 public datasets and 1 additional private dataset, expanding 22 surgical procedures, 11 surgical specialties, and relevant tasks, to construct the SurgBench. The full dataset description is shown in Table 2. Detailed surgical specialties and procedures are provided in Table 6. In contrast to existing work, which usually focuses on specific surgical types or diseases, we unify all of these datasets together, with the goal of building a comprehensive surgical video analysis dataset for more generalizable model performance. However, some datasets in SurgBench are released under licenses that do not allow for secondary distribution. Specifically, AVOS, SimSurgSkill2021, and AlxSuture are under

Source ID	Source Name	Disease Type	Procedures	Task Type	Pre-train Frames	Evaluation Frames
S1	AVOS (Goodman et al. (2024))	Multiple	Multiple, Open	Phase/Action/Inst cls.	28,473,879	–
S2	AlxSuture (Hoffmann et al. (2024))	N/A (Skills)	Tissue Suturing	GRS assessment	2,867,078	–
S3	Cholec80 (Yu et al. (2018))	Gallbladder	Cholecystectomy	Phase cls., Tool presence	4,612,530	–
S4	CholecT45 (Nwoye et al. (2022))	Gallbladder	Cholecystectomy	Action cls. (triplets)	74,855	–
S5	Colonoscopic	Colorectal lesions	GI diagnosis	Disease cls.	36,534	–
S6	Endo-FM (Wang et al. (2023b))	Various GI	Various Endoscopy	SSL tasks	3,646,432	–
S7	SimSurgSkill 2021	N/A (Simulation)	Liver/Abdominal (sim)	Skill metrics, Tool detection	1,248,156	–
S8	JIGSAWS (2017) (Ahmadi et al. (2017))	N/A (Skills)	Suture/Knot/Needle	Skill assessment, Gesture classification	569,048	537,645
S9	CholecT50 (Nwoye et al. (2022))	Gallbladder	Cholecystectomy	Action cls., Phase cls., Inst detection	90,444	207,169
S10	AutoLaparo (Wang et al. (2022))	Uterine	Hysterectomy	Phase cls., Motion prediction, Segmentation	2,155,843	160,221
S11	EndoVis 2019 (Wagner et al. (2021))	Gallbladder	Cholecystectomy	Phase/Action/Instrument cls., Skill assessment	4,501,791	1,176,000
S12	Hyper-Kvasir (Borgli et al. (2020))	GI pathologies	GI procedures	Tissue/Pathology segmentation, Classifica- tion	889,372	102,515
S13	Colonoscopic-web (Mesejo et al. (2016))	Colorectal lesions	GI diagnosis	Data augmentation	75,298	75,298
S14	Kvasir-Capsule (Smetsrud et al. (2021))	GI pathologies	GI screening	Pathology clas.	4,765,114	61,760
S15	LDPolypVideo (Ma et al. (2021))	Colonic polyps	Polyp screening	Polyp detection, Classification	878,487	543,777
S16	Private Data	Right colon ca.	Lap. Rt. Hemicolectomy	Phase cls., Skill/Quality assessment	1,138,833	816,952
Total					56,062,458	3,680,417

Table 2: Summary of the original sources comprising SurgBench Datasets, including publicly available academic datasets, medical competition datasets, demonstration data, and private data. Sources span different disease types, procedures, and task types. Sources above the dashed line do not provide labels and are only used to create SurgBench-P.

GI: Gastrointestinal; GRS: Global Rating Score; cls.: classification; sim: simulation; SSL: Self-supervised learning; Obj.: Object; ca.: cancer; Lap.: Laparoscopic; Rt.: Right; Inst.: Instrument

more restrictive licenses (e.g., CC-BY-NC-ND 4.0), which prohibit modification and redistribution. While these datasets were used in pretraining the model, they are not included in the SurgBench-E that we are releasing as the benchmark. Researchers wishing to use these datasets to pretrain the models should request access directly from the dataset providers. Ethical considerations and the original dataset licenses are fully outlined in the appendix A.

3.2 Dataset Preprocessing

Different surgical videos vary in coding format, FPS, video duration, spatial resolution, etc. To standardize data management and accelerate the training process, we perform a series of preprocessing and standardization steps across the 16 video sources. We standardize the videos with H.264 encoding, which offers the best compatibility with various processing libraries, significantly speeding up data loading in the training pipeline. The resolution is compressed to a minimum dimension of 320 (maintaining the aspect ratio, providing space for data augmentation, with the input resolution to the network set at 224x224), and the frame rate is unified to 20-30 FPS.

3.3 Dataset Formulation

For the format-standardized videos, pretraining and evaluation videos are processed differently. For pretraining data, we employed a fairly straightforward method to process the pre-training data by splitting the unlabelled videos into short clips lasting 10 seconds. For evaluation data, we implemented a series of measures to ensure the rationality and usability of benchmark clips. Firstly, we divide all the videos into short clips (lasting 1-10 seconds) with labels. Then, we split them into 5:5 training and testing sets. To prevent the model from focusing on background or scene-specific attributes unrelated to the label (Soomro et al., 2012), clips from the same video could only appear in either the training set or the test set. To prevent overly dominant or scarce labels from contaminating the benchmarks,

the IF (Imbalance Factor) is controlled within 10 through dynamically controlling the clip duration, down-sampling the samples from dominant labels, and removing scarce labels. As for one video corresponding to multiple labels, we split multi-label samples into multiple single-label samples and use the top-k accuracy metric. We have tested the efficacy of each dataset by fine-tuning VideoMAE (standard) on them, and the training dynamics are shown in Figure 2. The label distribution of training and testing videos is relatively close, exhibiting a long-tailed distribution, as shown in Figure 3. The details of processing steps in each dataset are provided in Appendix E.

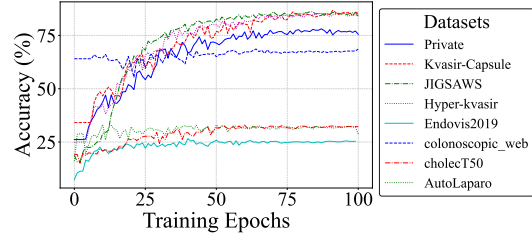


Figure 2: Fine-tuning performance on different source datasets, showing accuracy gains as training progresses. The consistently increasing accuracy curves validate the reliability and data quality of SurgBench-E.

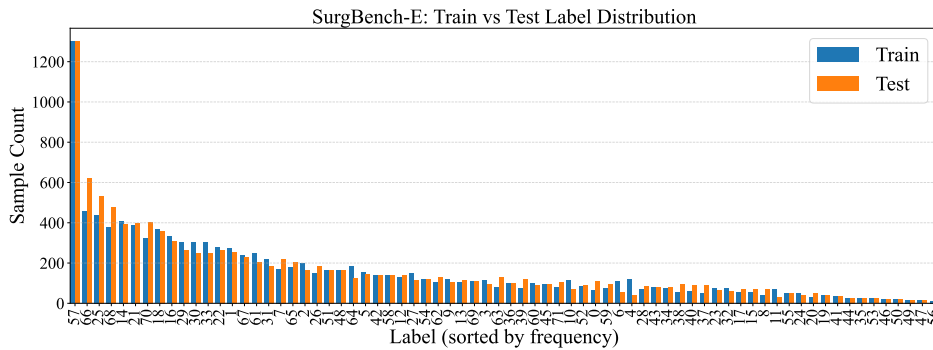


Figure 3: Training and test label distribution of SurgBench-E. The pronounced long-tail pattern aligns with real clinical scenarios, reflecting both authenticity and challenge. Label to task description is illustrated in Table 7.

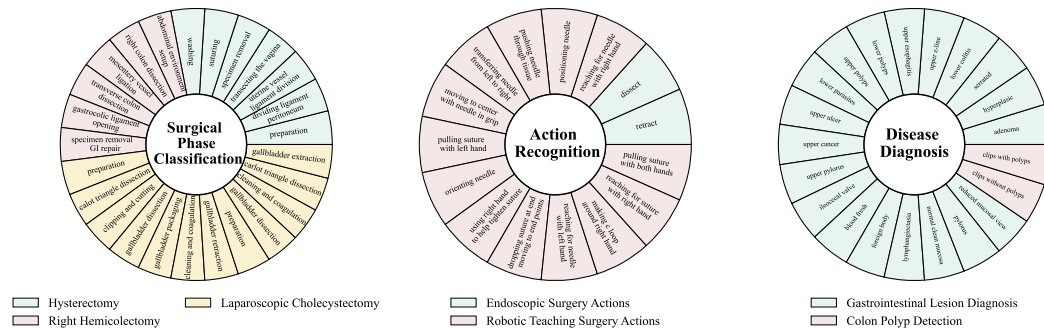


Figure 4: Pie charts of task in SurgBench-E. We have six categories, with three category distributions shown here. Different colors represent different sub-categories. The other three categories are provided in Appendix, Figure 9.

3.4 Benchmark statistics:

The whole SurgBench encompasses 225,250 clips of videos, 59,742,875 frames, lasting 575 hours with 22 surgical procedures and 11 specialties. SurgBench-E contains a total of 23,004 video clips and 72 fine-grained labels for facilitating fine-tuning and testing the model’s ability on a wide range of surgical tasks. We define a hierarchical taxonomy called **6C-10S-72T** on SurgBench-E with **6** Categories (three of them are illustrated in Figure 5, Figure 4) and **10** Sub-Categories with **72** detailed Tasks, as listed in Table 3. The sample distribution of the 10 sub-categories is naturally long-tailed,

as illustrated in Figure 1. The sample size is positively correlated to the number of labels in each category.

Category	Sub-Category (SC)	# Task	SC Code	Source ID
Phase Classification	Hysterectomy	7	T1	S10
	Right Hemicolectomy	6	T2	S16
	Laparoscopic Cholecystectomy	12	T3	S9, S11
Camera Motion	Camera Motion	7	T4	S10
Tool Recognition	Tool Recognition	2	T5	S9
Disease Diagnosis	Gastrointestinal Lesion Diagnosis	19	T6	S12, S13, S14
	Colon Polyp Detection	2	T7	S15
Action Classification	Endoscopic Surgery Actions	2	T8	S9
	Robotic Teaching Surgery Actions	13	T9	S8
Organ Detection	Organ Detection	2	T10	S9

Table 3: The **6C-10S-72T** taxonomy of our SurgBench-E. Source ID refers to the source of the dataset used in this task. SC codes used in Table 4.

4 Methodology

Continual pre-training We initiated our continual pre-training (CPT) by leveraging VideoMAE models (Tong et al., 2022) pre-trained on the general-domain Kinetics-400 dataset. The data used for pre-training, SurgBench-P (74.4 million frames total), **underwent a four-stage refinement** to ensure that it could learn general representations from large-scale data while aligning with downstream tasks. The training steps involved: (1) initial collection of all available videos into 225,250 clips; (2) filtering of less relevant or overly dominant large-scale samples (e.g., from AVOS); (3) applying upsampling for underrepresented data to encourage more IID learning; and (4) a final precise IID-oriented stage with both upsampling and downsampling. This culminated in a refined set of 39,807 video clips (resized to 224×224 resolution) for the final CPT phase. Following the VideoMAE methodology, we employed an asymmetric encoder-decoder architecture. The pre-training task involved reconstructing randomly masked spatiotemporal "tubes" of patches using an extremely high masking ratio of 0.9. CPT was performed for two VideoMAE variants: VideoMAE-Standard, which incorporates a ViT-Base encoder and a 4-layer Transformer decoder, and VideoMAE-Large, featuring a ViT-Large encoder paired with a 12-layer Transformer decoder. CPT parameters for both variants included an input of 16 frames per clip with a temporal sampling rate of 4. We utilized the AdamW optimizer ($\beta_1 = 0.9, \beta_2 = 0.95$). The effective batch size was 512 for the Base model (per-GPU batch of 64) and 256 for the Large model (per-GPU batch of 32). The resulting model is named SurgMAE-CPT (Standard version and Large version).

Fine-tuning: We finetune and test the SurgMAE-CPT on the SurgBench-E, the resulting model is called SurgMAE (standard and large). To validate the effectiveness of continual pre-training on the backbone feature extractor, we opt to train the classifier and analyze the training dynamics. We use AdamW optimizer ($\beta_1 = 0.9, \beta_2 = 0.99$) with a learning rate of $1e-3$, batch size of 64 for fine-tuning standard SurgMAE-CPT, whereas the large SurgMAE-CPT is trained with a learning rate of $2e-3$, batch size of 16.

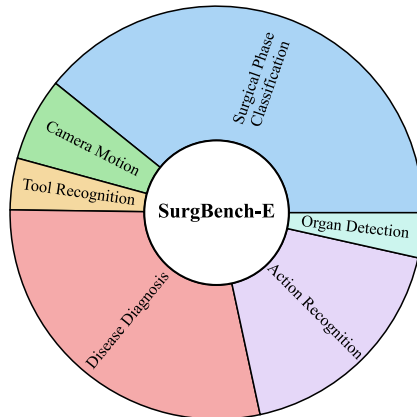


Figure 5: The pie chart of SurgBench-E, containing 6 categories and 72 tasks.

Task	Random Init.		VideoMAE		SurgMAE		SurgMAE(L)	
	Top-1	Top-3	Top-1	Top-3	Top-1	Top-3	Top-1	Top-3
T1	0.000	0.162	0.125	0.356	0.185	0.484	0.182	0.501
T2	0.364	0.667	0.423	0.777	0.440	0.818	0.493	0.856
T3	0.126	0.523	0.379	0.653	0.399	0.671	0.422	0.742
T4	0.000	0.000	0.298	0.629	0.293	0.628	0.306	0.645
T5	0.395	0.799	0.287	0.766	0.319	0.749	0.324	0.760
T6	0.413	0.605	0.569	0.744	0.645	0.838	0.666	0.905
T7	0.003	0.045	0.374	0.534	0.561	0.791	0.739	0.930
T8	0.000	0.044	0.005	0.254	0.015	0.383	0.020	0.411
T9	0.003	0.408	0.102	0.446	0.475	0.743	0.627	0.825
T10	0.000	0.290	0.122	0.632	0.200	0.575	0.279	0.695
Avg.	0.229	0.478	0.378	0.652	0.448	0.731	0.487	0.788

Table 4: Top-1 and Top-3 accuracy of models across tasks (T1–T10). Bold indicates best performance per task. The model is standard-sized except (L), which stands for large.

Training cost: For continual pre-training, the experiments were conducted on a cluster of 8 NVIDIA A100 GPUs. The VideoMAE-Base model was continually pre-trained for a total of 54 epochs on the surgical data, while the VideoMAE-Large model was trained for 38 epochs. The CPT process for both versions collectively took one week. For fine-tuning, we use one host with 8 RTX3090 (24 GB) GPUs. Both standard and large models are trained for 100 epochs, lasting 14 hours to converge.

5 Experiments and Results

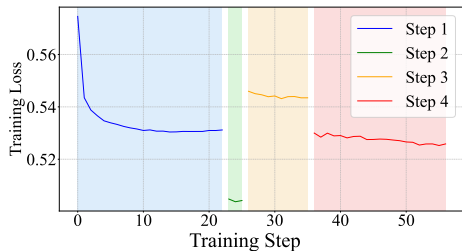
In this section, we present the experimental setup and results to validate the utility of SurgBench for surgical video analysis. We evaluate the performance of models trained using self-supervised pretraining with VideoMAE and fine-tuned on SurgBench-E. Our experiments focus on understanding training dynamics, model scalability, the impact of hyperparameters, generalization capabilities, and the benefits of continued pretraining.

5.1 Main Experiment Results

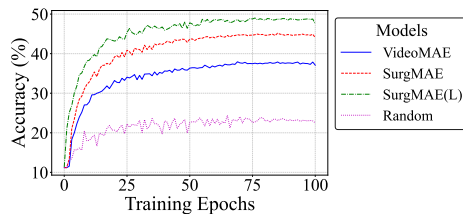
We conducted pre-training using the VideoMAE architecture on the SurgBench-P dataset (with all parameters fine-tuned) and further fine-tuned on SurgBench-E. The performance across 10 sub-categories is summarized in Table 4. To mitigate the interference caused by multiple categories present in a single sample, which can lead to unstable results, we considered both top-1 accuracy and top-3 accuracy. To compare the representational capacity of different backbones, we froze the feature extractor during fine-tuning and only trained the classification head.

The results show that continual pre-training on surgical videos has significantly improved accuracy on SurgBench-E, with consistent growth observed across metrics. Specifically, top-1 accuracy increased by 7% and top-3 accuracy by 7.9%. Most of the other sub-categories also showed noticeable improvement, except for T4 and T8, where the performance remained nearly unchanged. This suggests that the pre-training data has reliable quality and that self-supervised pre-training helps learn robust representations.

To gain a detailed understanding of which specific categories exhibit performance fluctuations on our pre-training and small task sets, we plotted the performance metrics for each category, as shown in Table ???. We identified two key patterns. First, the performance for a subset of categories is notably low. This is attributed to the scarcity of certain rare types in a few video domains, resulting in extremely limited data volume. This presents a challenge for future model optimization: how to achieve high performance for categories that are narrowly defined or underrepresented. Second, the pre-training process consistently improves the performance across nearly all individual categories, demonstrating the model’s robust generalization capability.



(a) Continuing pretraining dynamics of standard SurgMAE on SurgBench-P across 4 steps.



(b) Fine-tuning dynamics of different models on SurgBench-E. The model is standard-sized except SurgMAE(L), which stands for large version.

Figure 6: Dynamics of pretraining and fine-tuning on SurgBench. For pretraining, we track 4 steps progressing from large-scale data to small-scale distribution alignment with SurgBench-E. For fine-tuning, we compare randomly initialized weights, SurMAE pretrained on Kinetics, and large/standard versions pretrained on SurgBench-P. The stable decrease in loss curves and increase in accuracy demonstrate the rationality and quality of our dataset.

5.2 Training Dynamics

A stable training loss curve can strongly imply the quality of the data and the effectiveness of the training scheme. During pre-training, to evaluate the effectiveness of the data and training strategy, we analyzed the loss dynamics across four stages of progressive data distribution in the VideoMAE standard version. We find that within each stage, the loss decreases very smoothly, as seen in Figure 6. Moreover, due to differences in the difficulty and distribution of the training data, the transition of the loss values between different stages is not smooth. However, in actual task testing, this lack of smoothness does not negatively affect performance.

Furthermore, we observe that even though the loss curve in the final stage does not show a significant reduction, it still contributes to gradually stabilizing and improving the performance of task fine-tuning. This indicates that the model can continue representation learning even when the loss decreases more slowly.

Similarly, we also examined the quality of downstream task labels through training dynamics. We found that as the number of training epochs increases, the accuracy steadily rises. This phenomenon is consistent across the standard model, the large parameter model, the Kinetics pre-trained model, and the randomly initialized model.

5.3 Impact of Model Size on Performance

In language pre-training models, larger models with more parameters and scale typically exhibit better performance and stronger generalization capabilities. In the context of surgical foundation models, we also tested the performance of standard-sized and larger models on downstream tasks. As shown in Table 4, SurgMAE and SurgMAE(L) achieved a 3.9% increase in top-1 accuracy and a 5.7% increase in top-3 accuracy.

Furthermore, consistent growth was observed across task dimensions. This phenomenon is in line with the behavior of large-scale language models. Additionally, subsequent work on surgical procedure understanding suggests that further increasing the model scale can lead to even higher performance.

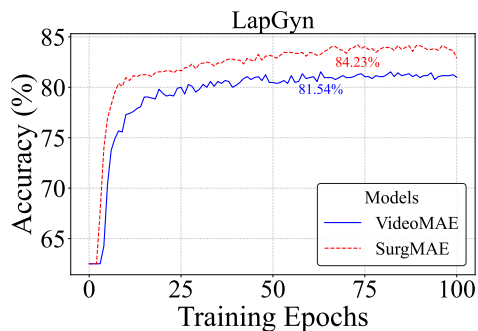


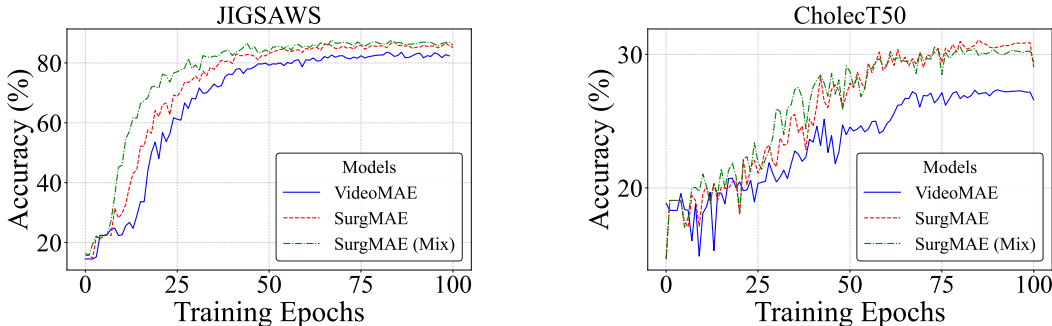
Figure 7: Performance on OOD dataset. We tested on the LapGyn task, which contains out-of-distribution data not seen during SurgBench-P training. The pre-trained model demonstrates superior convergence speed and final accuracy when fine-tuned on this out-of-domain downstream task.

5.4 Can Surg-FM generalize to unseen case?

Models trained on SurgBench can improve generalization across diverse distributions. We evaluated performance on datasets with varying degrees of similarity to SurgBench. Specifically, we tested on LapGyn4, a comprehensive dataset from gynecologic laparoscopic surgeries categorized into four distinct tasks (surgical actions, anatomical structures, actions on anatomy, and instrument count) (Leibetseder et al., 2018). We focused on an event recognition task in Laparoscopic Gynecology as described in (Nasirihaghighi et al., 2024). The fine-tuning dynamics are shown in Figure 7. Remarkably, models pretrained on SurgBench demonstrated significant performance gains of 2.69% even on this dissimilar distribution.

5.5 Data mix strategy between Pre-training and Fine-tuning

Data mixing during training significantly impacts downstream task performance. In SurgBench-P, we combined all source data for pre-training and used a strategy transitioning from "large-scale + unrestricted distribution" to "small-scale + aligned distribution." We hypothesize that optimal performance will follow as long as the training distribution aligns with the downstream task distribution in the final stage. Using the dataset (JIGSAWS and CholecT50) for both continuing pre-training on Kinetics-400 and fine-tuning, we observed that our model achieved superior convergence speed and final performance, seen in Figure 8.



(a) Fine-tuning dynamics of SurgMAE pretrained on mixed data. We first pretrained the model using a combined dataset of JIGSAWS and CholecT50, then fine-tuned it on JIGSAWS alone.

(b) Fine-tuning dynamics of SurgMAE on CholecT50. After pretraining on combined JIGSAWS and CholecT50 data, the model was fine-tuned specifically on the CholecT50 dataset.

Figure 8: Comparison of fine-tuning performance between models pretrained on mixed surgical data versus models trained from scratch, demonstrating the effectiveness of our data mixing strategy.

6 Conclusions

We present SurgBench, a comprehensive benchmark for surgical video understanding. Our contributions include: (1) SurgBench-P, a diverse pretraining dataset comprising 53 million frames across 22 surgical procedures and 11 surgical specialties; (2) SurgBench-E, a structured evaluation benchmark with 6 category, 10 sub-categories, and 72 fine-grained tasks, facilitating comprehensive surgical video benchmarking; and (3) empirical validation demonstrating significant performance gains through self-supervised learning on surgical videos. Experimental results show that models pretrained on SurgBench outperform those pretrained on natural video datasets. SurgBench provides a unified platform for surgical video analysis that will accelerate research progress in this domain.

7 Limitations

Despite its contributions, SurgBench has several limitations: (1) the long-tail class distribution challenges model training, requiring further research to improve minority class performance; (2) language supervision integration remains unexplored but potentially beneficial; and (3) optimal architectural designs for surgical video foundation models require additional investigation to maximize cross-task performance.

References

- Ahmidi, N., Tao, L., Sefati, S., Gao, Y., Lea, C., Haro, B. B., Zappella, L., Khudanpur, S., Vidal, R., and Hager, G. D. (2017). A dataset and benchmarks for segmentation and recognition of gestures in robotic surgery. *IEEE Transactions on Biomedical Engineering*, 64(9):2025–2041.
- Bar, O., Neimark, D., Zohar, M., Hager, G. D., Girshick, R., Fried, G. M., Wolf, T., and Asselmann, D. (2020). Impact of data on generalization of ai for surgical intelligence applications. *Scientific reports*, 10(1):22208.
- Bi, J., Wang, Y., Chen, H., Xiao, X., Hecker, A., Tresp, V., and Ma, Y. (2024). Visual instruction tuning with 500x fewer parameters through modality linear representation-steering. *arXiv preprint arXiv:2412.12359*.
- Bi, J., Wang, Y., Yan, D., Xiao, X., Hecker, A., Tresp, V., and Ma, Y. (2025). Prism: Self-pruning intrinsic selection method for training-free multimodal data selection. *arXiv preprint arXiv:2502.12119*.
- Borgli, H., Thambawita, V., Smedsrud, P. H., Hicks, S., Jha, D., Eskeland, S. L., Randel, K. R., Pogorelov, K., Lux, M., Nguyen, D. T. D., Johansen, D., Griwodz, C., Stensland, H. K., Garcia-Ceja, E., Schmidt, P. T., Hammer, H. L., Riegler, M. A., Halvorsen, P., and de Lange, T. (2020). HyperKvasir, a comprehensive multi-class image and video dataset for gastrointestinal endoscopy. *Scientific Data*, 7(1):283.
- Che, C., Wang, C., Vercauteren, T., Tsoka, S., and Garcia-Peraza-Herrera, L. C. (2025). Surg-3m: A dataset and foundation model for perception in surgical settings. *arXiv preprint arXiv:2503.19740*.
- Dimick, J. B. and Varban, O. A. (2015). Surgical video analysis: an emerging tool for improving surgeon performance.
- Fujii, R., Hatano, M., Saito, H., and Kajita, H. (2024). Egosurgery-phase: a dataset of surgical phase recognition from egocentric open surgery videos. In *International Conference on Medical Image Computing and Computer-Assisted Intervention*, pages 187–196. Springer.
- Goodman, E. D., Patel, K. K., Zhang, Y., Locke, W., Kennedy, C. J., Mehrotra, R., Ren, S., Guan, M., Zohar, O., Downing, M., et al. (2024). Analyzing surgical technique in diverse open surgical videos with multitask machine learning. *JAMA surgery*, 159(2):185–192.
- Green, J. L., Suresh, V., Bittar, P., Ledbetter, L., Mithani, S. K., and Allori, A. (2019). The utilization of video technology in surgical education: a systematic review. *journal of surgical research*, 235:171–180.
- Grenda, T. R., Pradarelli, J. C., and Dimick, J. B. (2016). Using surgical video to improve technique and skill. *Annals of surgery*, 264(1):32–33.
- Grüter, A. A., Van Lieshout, A. S., van Oostendorp, S. E., Henckens, S. P., Ket, J. C., Gisbertz, S. S., Toorenvliet, B. R., Tanis, P. J., Bonjer, H. J., and Tuynman, J. B. (2023). Video-based tools for surgical quality assessment of technical skills in laparoscopic procedures: a systematic review. *Surgical endoscopy*, 37(6):4279–4297.
- Guo, H., Ma, Z., Zeng, Z., Luo, M., Zeng, W., Tang, J., and Zhao, X. (2025). Each fake news is fake in its own way: An attribution multi-granularity benchmark for multimodal fake news detection. In *Proceedings of the AAAI Conference on Artificial Intelligence*, volume 39, pages 228–236.
- Hoffmann, H., Funke, I., Peters, P., Venkatesh, D. K., Egger, J., Rivoir, D., Röhrig, R., Hölzle, F., Bodenstedt, S., Willemer, M.-C., et al. (2024). Aixsuture: vision-based assessment of open suturing skills. *International Journal of Computer Assisted Radiology and Surgery*, 19(6):1045–1052.
- Leibetseder, A., Petscharnig, S., Primus, M. J., Kletz, S., Münzer, B., Schoeffmann, K., and Keckstein, J. (2018). Lapgyn4: a dataset for 4 automatic content analysis problems in the domain of laparoscopic gynecology. In *Proceedings of the 9th ACM Multimedia Systems Conference, MMSys 2018, Amsterdam, The Netherlands, June 12-15, 2018*, pages 357–362. ACM.
- Levin, M., McKechnie, T., Khalid, S., Grantcharov, T. P., and Goldenberg, M. (2019). Automated methods of technical skill assessment in surgery: a systematic review. *Journal of surgical education*, 76(6):1629–1639.
- Li, J., Skinner, G., Yang, G., Quaranto, B. R., Schwaitzberg, S. D., Kim, P. C., and Xiong, J. (2024). Llava-surg: towards multimodal surgical assistant via structured surgical video learning. *arXiv preprint arXiv:2408.07981*.
- Li, K., Wang, Y., Li, Y., Wang, Y., He, Y., Wang, L., and Qiao, Y. (2023). Unmasked teacher: Towards training-efficient video foundation models. In *Proceedings of the IEEE/CVF International Conference on Computer Vision*, pages 19948–19960.
- Li, Y., He, H., Cao, Y., Cheng, Q., Fu, X., and Tang, R. (2025a). M2iv: Towards efficient and fine-grained multimodal in-context learning in large vision-language models. *arXiv preprint arXiv:2504.04633*.

- Li, Y., Yang, J., Li, B., and Tang, R. (2025b). Cama: Enhancing multimodal in-context learning with context-aware modulated attention. *arXiv preprint arXiv:2505.17097*.
- Li, Y., Yun, T., Yang, J., Feng, P., Huang, J., and Tang, R. (2025c). Taco: Enhancing multimodal in-context learning via task mapping-guided sequence configuration. *arXiv preprint arXiv:2505.17098*.
- Loftus, T. J., Filiberto, A. C., Li, Y., Balch, J., Cook, A. C., Tighe, P. J., Efron, P. A., Upchurch Jr, G. R., Rashidi, P., Li, X., et al. (2020). Decision analysis and reinforcement learning in surgical decision-making. *Surgery*, 168(2):253–266.
- Ma, Y., Chen, X., Cheng, K., Li, Y., and Sun, B. (2021). Ldpolypvideo benchmark: a large-scale colonoscopy video dataset of diverse polyps. In *Medical Image Computing and Computer Assisted Intervention—MICCAI 2021: 24th International Conference, Strasbourg, France, September 27–October 1, 2021, Proceedings, Part V 24*, pages 387–396. Springer.
- Ma, Z., Luo, M., Guo, H., Zeng, Z., Hao, Y., and Zhao, X. (2024). Event-radar: Event-driven multi-view learning for multimodal fake news detection. In *Proceedings of the 62nd Annual Meeting of the Association for Computational Linguistics (Volume 1: Long Papers)*, pages 5809–5821.
- Madan, N., Møgelmoose, A., Modi, R., Rawat, Y. S., and Moeslund, T. B. (2024). Foundation models for video understanding: A survey. *Authorea Preprints*.
- Mesejo, P., Pizarro, D., Abergel, A., Rouquette, O., Beorchia, S., Poincloux, L., and Bartoli, A. (2016). Computer-aided classification of gastrointestinal lesions in regular colonoscopy. *IEEE transactions on medical imaging*, 35(9):2051–2063.
- Misawa, M., Kudo, S.-e., Mori, Y., Hotta, K., Ohtsuka, K., Matsuda, T., Saito, S., Kudo, T., Baba, T., Ishida, F., et al. (2021). Development of a computer-aided detection system for colonoscopy and a publicly accessible large colonoscopy video database (with video). *Gastrointestinal endoscopy*, 93(4):960–967.
- Nasirihaghighi, S., Ghamsarian, N., Husslein, H., and Schoeffmann, K. (2024). Event recognition in laparoscopic gynecology videos with hybrid transformers. In *MultiMedia Modeling (MMM 2024)*, pages 82–95. Springer.
- Nwoye, C. I., Yu, T., Gonzalez, C., Seeliger, B., Mascagni, P., Mutter, D., Marescaux, J., and Padoy, N. (2022). Rendezvous: Attention mechanisms for the recognition of surgical action triplets in endoscopic videos. *Medical Image Analysis*, 78:102433.
- Prebay, Z. J., Peabody, J. O., Miller, D. C., and Ghani, K. R. (2019). Video review for measuring and improving skill in urological surgery. *Nature Reviews Urology*, 16(4):261–267.
- Schmidgall, S., Kim, J. W., Jopling, J., and Krieger, A. (2024). General surgery vision transformer: A video pre-trained foundation model for general surgery. *arXiv preprint arXiv:2403.05949*.
- Smedsrud, P. H., Thambawita, V., Hicks, S. A., Gjestang, H., Nedrejord, O. O., Næss, E., Borgli, H., Jha, D., Berstad, T. J. D., Eskeland, S. L., Lux, M., Espeland, H., Petlund, A., Nguyen, D. T. D., Garcia-Ceja, E., Johansen, D., Schmidt, P. T., Toth, E., Hammer, H. L., de Lange, T., Riegler, M. A., and Halvorsen, P. (2021). Kvasir-Capsule, a video capsule endoscopy dataset. *Scientific Data*, 8(1):142.
- Soomro, K., Zamir, A. R., and Shah, M. (2012). Ucf101: A dataset of 101 human actions classes from videos in the wild.
- Tong, Z., Song, Y., Wang, J., and Wang, L. (2022). Videomae: Masked autoencoders are data-efficient learners for self-supervised video pre-training. *Advances in neural information processing systems*, 35:10078–10093.
- Twinanda, A. P., Shehata, S., Mutter, D., Marescaux, J., De Mathelin, M., and Padoy, N. (2016). Endonet: a deep architecture for recognition tasks on laparoscopic videos. *IEEE transactions on medical imaging*, 36(1):86–97.
- Wagner, M., Müller-Stich, B.-P., Kisilenko, A., Tran, D., Heger, P., Mündermann, L., Lubotsky, D. M., Müller, B., Davitashvili, T., Capek, M., Reinke, A., Yu, T., Vardazaryan, A., Nwoye, C. I., Padoy, N., Liu, X., Lee, E.-J., Disch, C., Meine, H., Xia, T., Jia, F., Kondo, S., Reiter, W., Jin, Y., Long, Y., Jiang, M., Dou, Q., Heng, P. A., Twick, I., Kirtac, K., Hosgor, E., Bolmgren, J. L., Stenzel, M., von Siemens, B., Kennigott, H. G., Nickel, F., von Frankenberg, M., Mathis-Ullrich, F., Maier-Hein, L., Speidel, S., and Bodenstedt, S. (2021). Comparative validation of machine learning algorithms for surgical workflow and skill analysis with the heichole benchmark.
- Wang, G., Bai, L., Wang, J., Yuan, K., Li, Z., Jiang, T., He, X., Wu, J., Chen, Z., Lei, Z., et al. (2025). Endochat: Grounded multimodal large language model for endoscopic surgery. *arXiv preprint arXiv:2501.11347*.

- Wang, L., Huang, B., Zhao, Z., Tong, Z., He, Y., Wang, Y., Wang, Y., and Qiao, Y. (2023a). Videomae v2: Scaling video masked autoencoders with dual masking. In *Proceedings of the IEEE/CVF conference on computer vision and pattern recognition*, pages 14549–14560.
- Wang, Y., Li, K., Li, X., Yu, J., He, Y., Chen, G., Pei, B., Zheng, R., Wang, Z., Shi, Y., et al. (2024). Internvideo2: Scaling foundation models for multimodal video understanding. In *European Conference on Computer Vision*, pages 396–416. Springer.
- Wang, Z., Liu, C., Zhang, S., and Dou, Q. (2023b). Foundation model for endoscopy video analysis via large-scale self-supervised pre-train. In *International Conference on Medical Image Computing and Computer-Assisted Intervention*, pages 101–111. Springer.
- Wang, Z., Lu, B., Long, Y., Zhong, F., Cheung, T.-H., Dou, Q., and Liu, Y. (2022). Autolaparo: A new dataset of integrated multi-tasks for image-guided surgical automation in laparoscopic hysterectomy. In *International Conference on Medical Image Computing and Computer-Assisted Intervention*, pages 486–496. Springer.
- Yu, T., Mutter, D., Marescaux, J., and Padoy, N. (2018). Learning from a tiny dataset of manual annotations: a teacher/student approach for surgical phase recognition. *arXiv preprint arXiv:1812.00033*.
- Zeng, Z., Luo, M., Kong, X., Liu, H., Guo, H., Yang, H., Ma, Z., and Zhao, X. (2024). Mitigating world biases: A multimodal multi-view debiasing framework for fake news video detection. In *Proceedings of the 32nd ACM International Conference on Multimedia*, pages 6492–6500.
- Zhang, B., Li, K., Cheng, Z., Hu, Z., Yuan, Y., Chen, G., Leng, S., Jiang, Y., Zhang, H., Li, X., et al. (2025). Videollama 3: Frontier multimodal foundation models for image and video understanding. *arXiv preprint arXiv:2501.13106*.
- Zhao, L., Gundavarapu, N. B., Yuan, L., Zhou, H., Yan, S., Sun, J. J., Friedman, L., Qian, R., Weyand, T., Zhao, Y., et al. (2024). Videoprism: A foundational visual encoder for video understanding. *arXiv preprint arXiv:2402.13217*.
- Zhou, C., Jiang, R., Luan, F., Meng, S., Wang, Z., Dong, Y., Zhou, Y., and He, B. (2025a). Dual-arm robotic fabric manipulation with quasi-static and dynamic primitives for rapid garment flattening. *IEEE/ASME Transactions on Mechatronics*.
- Zhou, C., Xu, H., Hu, J., Luan, F., Wang, Z., Dong, Y., Zhou, Y., and He, B. (2025b). Ssfold: Learning to fold arbitrary crumpled cloth using graph dynamics from human demonstration. *IEEE Transactions on Automation Science and Engineering*.

A Dataset License

SurgBench aggregates several publicly available surgical video datasets, with their respective licenses meticulously reviewed to ensure compliant use within the research community. The core components of SurgBench, intended for direct benchmarking and fine-tuning, primarily consist of datasets released under licenses permitting academic and non-commercial research, such as Cholec80 (CC-BY-NC-SA 4.0), Kvasir-Capsule (custom academic/educational use), and SUN-SEG (custom non-commercial research use over Apache License). Notably, while foundational models developed alongside SurgBench were pre-trained using a broader corpus that included datasets with more restrictive terms like AVOS, SimSurgSkill2021, and AIxSuture (CC-BY-NC-ND 4.0), these specific datasets are not redistributed as part of SurgBench’s fine-tuning suite due to their licensing limitations (e.g., challenge-specific, no derivatives). Users are strongly encouraged to consult the original sources for comprehensive licensing details of each constituent dataset.

B Pie chart of other three categories

The pie chart of the camera motion, organ detection, tool recognition is shown in Figure 9.

C Pretraining Data Composition

The composition of pretraining data is shown in Table 6,

Dataset Name	License Type	Usage Conditions
Datasets for SurgBench-P and SurgBench-E		
Cholec80	CC-BY-NC-SA 4.0	Attribution required, non-commercial use, share-alike
Hyper-Kvasir	Custom	Citation required, academic use
Kvasir-Capsule	Custom	Attribution required, research and educational purposes
Colonoscopic Dataset	Custom	Publicly available, registration required
AutoLaparo	CC-BY-NC-SA 4.0	Attribution required, non-commercial use, share-alike
SUN-SEG	Custom	Application required, research and educational purposes
CholecT50	CC-BY-NC-SA 4.0	Attribution required, non-commercial use, share-alike
JIGSAWS	Custom	Application required, academic research, specific citations
Endoscopic Vision 2019	Custom	Form submission required, academic use
Datasets For SurgBench-P Only		
SimSurgSkill2021	Challenge-specific	Limited to challenge scope only
AVOS	Custom protocol	Redistribution prohibited, academic research only
AIxSuture	CC-BY-NC-ND 4.0	Modifications and commercial use prohibited

Table 5: Classification of Surgical Datasets by License

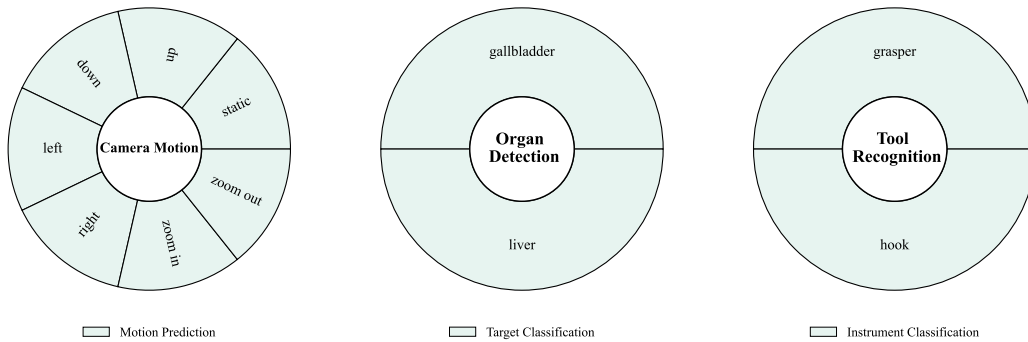


Figure 9: Pie charts of task in SurgBench-E. We have six categories, with three category distributions shown here. Different colors represent different sub-categories.

Clinical Specialty	Surgical Procedure	Source ID
General Surgery	Appendectomy	S1, S6
General Surgery	Cholecystectomy	S1, S3, S4, S9, S11
General Surgery	Gastrectomy	S1, S6
General Surgery	Hernia Repair	S1, S6
General Surgery	Splenectomy	S1, S7
General Surgery	Pilonidal cystectomy	S1
General Surgery	Bariatric surgery	S1, S6
General Surgery	Anti-reflux surgery	S1, S12
General Surgery	Hepatectomy	S1, S6, S7
Colon and Rectal Surgery	Colectomy	S1, S6, S12, S16
Colon and Rectal Surgery	Colostomy	S1, S6, S12
Thoracic Surgery	Esophagectomy	S1, S6, S12
Urological Surgery	Nephrectomy	S1
Urological Surgery	Adrenalectomy	S1
Obstetrics and Gynecology	Hysterectomy	S1, S10
Obstetrics and Gynecology	Gynecologic Oncology	S1, S10
Neurological Surgery	Neurological Surgery	S1
Ophthalmic Surgery	Ophthalmic Surgery	S1
Oral and Maxillofacial Surgery	Oral and Maxillofacial Surgery	S1
Orthopaedic Surgery	Orthopaedic Surgery	S1
Otolaryngology	Otolaryngology	S1
Pediatric Surgery	Pediatric Surgery	S1

Table 6: Clinical specialties and surgical procedures and their sources (ID) of SurBennch-P

D Label to task mapping

The 72 label to task mapping is shown in Table 7, 8.

Label	Description
0	surgical_phase-preparation
1	surgical_phase-dividing_ligament_and_peritoneum
2	surgical_phase-dividing_uterine_vessels_and_ligament
3	surgical_phase-transecting_the_vagina
4	surgical_phase-specimen_removal
5	surgical_phase-suturing
6	surgical_phase-washing
7	motion_prediction-static
8	motion_prediction-up
9	motion_prediction-down
10	motion_prediction-left
11	motion_prediction-right
12	motion_prediction-zoom-in
13	motion_prediction-zoom-out
14	instrument_classification-grasper
15	instrument_classification-hook
16	verb_classification-retract
17	verb_classification-dissect
18	target_classification-gallbladder
19	target_classification-liver
20	phase_classification-preparation
21	phase_classification-carlot-triangle-dissection
22	phase_classification-gallbladder-dissection
23	phase_classification-cleaning-and-coagulation
24	phase_classification-gallbladder-extraction
25	disease_classification-adenoma
26	disease_classification-hyperplasic
27	disease_classification-serrated
28	phase_classification-preparation
29	phase_classification-calot_triangle_dissection
30	phase_classification-clipping_and_cutting
31	phase_classification-galbladder_dissection
32	phase_classification-galbladder_packaging
33	phase_classification-cleaning_and_coagulation
34	phase_classification-galbladder_retraction
35	disease_classification-home
36	disease_classification-home
37	disease_classification-home

Table 7: Label Descriptions (Part 1)

E Details of processing steps in each dataset

Private Data The dataset used in this study is derived from laparoscopic right hemicolectomy procedures and focuses on surgical phase classification. The original dataset consists of surgical videos collected from **three tertiary grade A hospitals** in China. These videos were initially stored in their raw format, organized under a hierarchical directory structure corresponding to different surgical phases as outlined in the Competency Assessment Tool (CAT) for laparoscopic right hemicolectomy. The primary data components include six distinct phases: 1. Establishment of abdominal surgical environment, 2. Dissection of the posterior peritoneal space of the right colon and the right hemi-colon, 3. Identification and ligation of the vessels on the mesentery, 4. Dissection of the posterior

Label	Description
38	disease_classification-home
39	disease_classification-home
40	disease_classification-home
41	disease_classification-home
42	disease_classification-home
43	disease_classification-home
44	gesture_classification-reaching_for_needle_with_right_hand
45	gesture_classification-positioning_needle
46	gesture_classification-pushing_needle_through_tissue
47	gesture_classification-transferring_needle_from_left_to_right
48	gesture_classification-moving_to_center_with_needle_in_grip
49	gesture_classification-pulling_suture_with_left_hand
50	gesture_classification-orienting_needle
51	gesture_classification-using_right_hand_to_help_tighten_suture
52	gesture_classification-dropping_suture_at_end_and_moving_to_end_points
53	gesture_classification-reaching_for_needle_with_left_hand
54	gesture_classification-making_c_loop_around_right_hand
55	gesture_classification-reaching_for_suture_with_right_hand
56	gesture_classification-pulling_suture_with_both_hands
57	disease_classification-ileocecal_valve
58	disease_classification-blood-fresh
59	disease_classification-foreign-body
60	disease_classification-lymphangiectasia
61	disease_classification-normal-clean-mucosa
62	disease_classification-pylorus
63	disease_classification-reduced-mucosal-view
64	polyp_detection-clips_without_polyps
65	polyp_detection-clips_with_polyps
66	phase_classification-1_establishment_of_abdominal_surgical_environment
67	phase_classification-2_dissection_of_the_posterior_peritoneal_space
68	phase_classification-3_identification_and_ligation_of_the_vessels_on_the_mesentery
69	phase_classification-4_dissection_of_the_posterior_peritoneal_space
70	phase_classification-5_opening_of_the_gastrocolic_ligament_and_identification
71	phase_classification-6_specimen_removal_and_gastrointestinal_reconstruction_(intra-abdominal_and_extra-abdominal_anastomosis)

Table 8: Label Descriptions (Part 2)

peritoneal space of the transverse colon and the Henle’s trunk, 5. Opening of the gastrocolic ligament and identification of the mesenteric interspace (IMS), and 6. Specimen removal and gastrointestinal reconstruction (intra-abdominal and extra-abdominal anastomosis). Each video was annotated with detailed metadata regarding exposure, adverse events, technical operations, and quality evaluations, enabling a comprehensive assessment of surgical proficiency.

To prepare the dataset for machine learning tasks, we implemented a systematic preprocessing pipeline using Python scripts. The raw videos were segmented into 30-second clips, which were then accelerated by a factor of 3 to compress each clip into 10 seconds while preserving the essential visual information. This process utilized the `ffmpeg` library, ensuring precise frame-level extraction and efficient compression. The segmentation logic involved calculating the total video duration using `ffprobe`, dividing it into non-overlapping intervals, and applying a single filter chain for both video and audio streams to maintain synchronization. Clips were saved in the H.264 codec with AAC audio encoding, optimized for fast network streaming using the `+faststart` flag. Metadata for each clip, including its label, relative path, compressed duration, and associated task type, was recorded in a JSON file for subsequent model training.

After processing, the dataset was divided into N clips across the six categories, with each clip having a standardized duration of approximately 10 seconds. The resolution of the videos was preserved at 1920×1080 pixels, with a frame rate of 30 frames per second (fps). The total number of frames

across all clips amounted to approximately $30 \times N$, providing a rich resource for temporal modeling. The private data, is structured hierarchically, with each clip labeled according to its surgical phase, enabling supervised learning approaches for phase recognition. The final metadata file, containing detailed annotations for each clip, was saved in JSON format.

AutoLaparo The AutoLaparo is a multi-task dataset specifically designed for advancing image-guided surgical automation in laparoscopic hysterectomy. The original dataset comprises three main tasks: surgical workflow recognition (Task 1), laparoscope motion prediction (Task 2), and instrument and key anatomy segmentation (Task 3). Task 1 includes 21 laparoscopic hysterectomy videos, each annotated at 1 fps with seven surgical phases, while Task 2 consists of 300 video clips, each lasting 10 seconds, annotated with seven laparoscopic motion labels. Task 3 provides 1800 images with corresponding masks, annotated for four types of surgical instruments and one key anatomy. The dataset is organized into specific directories: Task 1 videos and labels are stored in `task1/videos` and `task1/labels`, respectively; Task 2 clips and their labels are located in `task2/clips` and `task2/laparoscope_motion_label.txt`; and Task 3 images and masks are stored in `task3/images` and `task3/masks`. For preprocessing, Task 1 videos are segmented into clips of 100 frames each, ensuring a consistent clip length, while Task 2 clips are directly used as provided. The dataset is split into training, validation, and testing sets: for Task 1, videos 01-10 are used for training, 11-14 for validation, and 15-21 for testing; for Task 2 and Task 3, clips 001-170 are designated for training, 171-227 for validation, and 228-300 for testing. Post-processing, the dataset contains 1,388 minutes of video, with a frame rate of 25 fps and a resolution of 1920×1080 pixels. This meticulous division ensures a balanced and representative dataset for robust model training and evaluation, facilitating comprehensive benchmarking in surgical automation tasks.

Cholec80 The Cholec80 dataset, originating from the University Hospital of Strasbourg/IRCAD, is a comprehensive collection of laparoscopic cholecystectomy videos designed for surgical workflow analysis. This dataset includes 80 high-resolution videos, each annotated with detailed phase labels and tool presence information, making it a valuable resource for research in surgical video understanding. The dataset's homepage (<http://camma.u-strasbg.fr/datasets>) provides an overview of its applications, including phase recognition and tool detection tasks. Additionally, the accompanying README file and annotations offer insights into the data structure, licensing, and citation requirements.

Initially, the dataset comprises 80 videos recorded at 25 frames per second (fps), with resolutions varying across videos. Each video is accompanied by two types of annotations: phase annotations and tool annotations. The phase annotations provide frame-level labels for seven surgical phases, including preparation, Calot triangle dissection, clipping and cutting, gallbladder dissection, gallbladder packaging, cleaning and coagulation, and gallbladder retraction. Tool annotations, sampled at 1 fps, indicate the presence or absence of seven surgical tools, such as graspers, bipolar devices, hooks, scissors, clippers, irrigators, and specimen bags. These annotations are stored in tab-separated text files, with frame indices and corresponding labels. Furthermore, timestamped phase annotations are provided to facilitate visualization during video playback.

To enable efficient processing and analysis, the dataset was preprocessed into shorter video clips. Each video was divided into non-overlapping clips of approximately 300 frames, corresponding to 12 seconds per clip at the original frame rate of 25 fps. This segmentation ensures manageable clip durations while preserving sufficient temporal context for downstream tasks. For each clip, phase and tool annotations were analyzed to determine dominant labels. Specifically, the most frequently occurring phase label within a clip was assigned as the clip's phase classification label, while tool presence was determined based on the maximum occurrence of each tool across frames. The resulting clips were saved in MP4 format using FFmpeg, maintaining the original resolution and frame rate. The preprocessing pipeline also generated metadata in JSON format, detailing clip paths, durations, and associated labels.

After preprocessing, the dataset consists of approximately 670 video clips, with a total duration of around 80 minutes. Each clip retains the original resolution and frame rate of 25 fps, ensuring consistency with the raw videos. The average clip length is 12 seconds, with slight variations due to the alignment of clip boundaries with video lengths. The resulting dataset is well-suited for training and evaluating models for surgical phase recognition and tool presence detection, offering a balanced distribution of surgical phases and tool usage patterns. This structured representation facilitates

the development of deep learning models tailored to laparoscopic video analysis, contributing to advancements in computer-assisted surgery.

Colonoscopic-web Colonoscopic-Web dataset contains 76 videos from colonoscopies documenting different types of gastrointestinal lesions. Each video is accompanied by annotated real data, including histopathologic findings, expert annotations, and calibration data from the recording system. Three categories, Adenoma, Hyperplastic and Serrated, were included in the dataset, representing the distribution of common polyp types. Long videos were cut into short 2-minute videos. The dataset is intended for use in studies of automated lesion detection and classification, with the goal of improving diagnostic accuracy and reducing the workload of clinicians by reducing the reliance on pigmented endoscopy in routine examinations.

Endovis2019 Endovis2019 dataset contains endoscopic video data from general surgical operating rooms, which were acquired during laparoscopic procedures at Heidelberg University Hospital and its affiliated hospitals. All surgeries were labeled frame-by-frame by surgical experts, and the labels include the phase of the surgery, surgical action, and instrument used. The recorded surgeries were mainly laparoscopic cholecystectomies. The dataset contains recorded videos of 30 different surgeries from at least three hospitals, and endoscopically captured videos of each procedure are provided. To ensure privacy, all additional extra-abdominal footage was masked by completely white frames. Tasks for this dataset include phase recognition, action classification, and tool classification. The phase recognition task entails classification based on the different stages of the surgical procedure. The dataset is labeled with a number of different stages ranging from the preparation stage to gallbladder traction. The action classification task involves categorizing surgical manipulation actions, including grasping, holding, cutting, and clipping actions. The instrument classification task required the classification of various tools used in surgery, covering a wide range of surgical instruments, like grasper, clipper, coagulation instruments, scissors, suction-irrigation, specimen bag and stapler. In addition, an “undefined instrument shaft” category was defined to label tools that are not explicitly categorized. Based on the label of each frame, the video is cut by frame classification, consecutive frames with the same label form a new video segment, and each new video segment is subsequently cut into 10-second videos.

hyper-kvasir Hyper-Kvasir dataset is a gastrointestinal image and video dataset of 374 gastroenteroscopy and colonoscopy videos from Bærum Hospital, Norway, totaling 11.62 hours and more than 1 million frames. This dataset was categorized according to a hierarchical structure. First, the dataset was categorized with the Upper GI and Lower GI as the first tier. The data were then subdivided according to four main categories, which included anatomical landmarks, pathological findings, quality of mucosal views, and therapeutic interventions, which formed the second tier. These categories were further subdivided into 30 specific subcategories that belonged to the third tier. By combining these subcategories with labels for the upper and lower GI tract, each video is given a new label. And each long video was cut into small 5-second video clips based on its categorization and stored in the corresponding folder. In addition, the dataset contains 10,662 annotated images in JPEG format with images labeled in 23 different lesion types covering a wide range of normal and pathologic manifestations in different parts of the gastrointestinal tract. These images and videos provide a large amount of training data for the development of an AI-assisted gastrointestinal endoscopy analysis system, and can especially help researchers cope with the category imbalance problem that is common in medical data.

kvasir-capsule Kvasir-Capsule dataset is an open dataset for gastrointestinal endoscopic video analysis. The dataset contains 4,741,621 pieces of data, including 47,238 labeled images with bounding boxes, 43 labeled videos, and 74 unlabeled videos. In addition, 4,694,266 unlabeled images can be extracted from all videos. The labeled images in the dataset are extracted from frames in the original long video. Based on the information of these labeled frames, the original video was cut into short videos every 5 seconds and kept consistent with the labels of the original long video. There were 47,238 labeled images in the dataset, which were classified into 14 different categories and divided into two main categories, Anatomy and Luminal findings. The Anatomy includes anatomical landmarks associated with the gastrointestinal tract, such as the pylorus, ileocecal valve, and ampulla of Vater, while the Luminal findings covers pathologic changes occurring in the gastrointestinal tract, such as Normal clean mucosa, reduced mucosal view, blood-fresh, blood-hematin, and so on. These images are widely used to study gastrointestinal diseases and help improve the diagnostic accuracy of endoscopy. At the same time, due to the imbalance in the number of images of various diseases in the dataset, especially for some of the rarer diseases, researchers need to employ effective machine

learning methods that are able to learn from the limited training data, especially for the recognition of rare diseases.

CholecT50 CholecT50 is a dataset of endoscopic videos of laparoscopic cholecystectomy procedures for fine-grained action recognition, designed to facilitate research on action recognition techniques in laparoscopic surgery. The dataset contains 45 videos from the Cholec80 dataset and 5 videos from the internal dataset Cholec120, all of which are finely labeled with the triad of information (<instrument, verb, target>) for each surgical action as well as the corresponding stage labels. The dataset also provides the spatial annotation of the instrument tips (bounding boxes) in the 5 videos and the frame-triad matching labels in all videos. In addition, each frame in the videos was extracted at a frequency of 1 frame per second and annotated with detailed surgical movements, aiming to support the study of movement recognition algorithms in laparoscopic surgery. The dataset was split into four tasks: phase classification, instrument classification, verb classification and target classification. The task division is based on the JSON annotation document for each frame, and each frame is labeled in detail, with several consecutive frames having the same label. To accommodate model training, all video clips are segmented into several short videos of 5 seconds with a frame rate of 10, and the labels are rearranged to map the labels of the four tasks to the range of 0-31 in order to uniformly standardize the training data.

LDPolyVideo LDPolyVideo dataset is a large and diverse dataset of colonoscopic polyp detection. It contains colonoscopy videos collected from routine clinical colonoscopies with all patient-related metadata removed. The dataset contains 160 videos totaling 40,266 frames, of which 33,884 frames contain polyps. To increase the diversity of the dataset, the data includes not only clear images of polyps, but also covers motion blurring due to camera movement, bowel folding and bowel peristalsis. The dataset was divided into training, validation and test sets. The images in the validation and test sets were labeled to indicate whether each frame contained a polyp or not, with a label value of 0 or 1, respectively. For these frames, the video is synthesized into video clips with fps of 25 and cut into short 5-10 second segments based on the frame-level labels. The training set is then divided based on the labeling of the entire video, containing videos with polyps and videos without polyps. For videos with polyps, the video is split evenly into 2 to 4 segments and each segment is compressed into a 10-second video to ensure that polyps are contained within each segment. For videos without polyps, the videos were cut into short segments of 5 to 10 seconds. This treatment ensures that each segment is correctly labeled and improves the diversity of the dataset and the generalization ability of the model.

JIGSAWS JIGSAWS dataset for modeling surgical activity in human motion was collected by Johns Hopkins University in collaboration with Intuitive Surgical. The dataset was collected using the da Vinci Surgical System from eight surgeons of varying skill levels, who performed five repetitions of three basic surgical tasks: suturing, knotting, and threading, which are standard components of most surgical skills training courses, on a tabletop model. The JIGSAWS dataset is comprised of three main components: the first component is kinematic data, which includes data that describes the operator's movement in terms of Cartesian positions, orientations, velocities, angular velocities and gripper angle describing the motion of the manipulators.; the second component is video data using stereoscopic video; and the third component is manually labeled data that includes gestures and skills. The dataset contains 15 labeled gestures in total, each corresponding to a specific task segment during surgery. The specific 15 labels include *G1*: "grasping the needle with the right hand", *G2*: "positioning the needle", *G3*: "passing the needle through the tissue", *G4*: "passing the needle from the left hand to right hand", *G5*: "Grasp the needle and move to the center", *G6*: "Pull the suture with the left hand", *G7*: "Pull the suture with the right hand", *G8*: "Adjust the direction of the needle", *G9*: "Use your right hand to help tighten the stitch", *G10*: "Loosen more stitches", *G11*: "Drop the stitch and move to the end", *G12*: "Grab the needle with your left hand", *G13*: "Make a C-shape around your right hand", *G14*: "Grab the seam allowance with your right hand", *G15*: "Pull the stitch with both hands". This labeling information was stored in a transcription file for each task, which consisted of threading the needle, sewing, and tying the knot.

AlxSuture AlxSuture dataset was collected to analyze the effectiveness of training guided by virtual reality head-mounted displays. It contains 314 videos documenting students performing open surgical suturing in a simulated environment and categorizing them into proficient, novice, and intermediate categories based on skill scores. Skills were scored using the Objective Structured Assessment of Technical Skills scale, with eight skill categories, and the sum of the scores from all categories formed a global rating GRS ranging from 8 to 40. Mean values were obtained through a preliminary analysis

of the pairwise Pearson correlation coefficients between the scores of the three assessors. For each video, the ratings of the three assessors were averaged and then categorized into three categories: novice, intermediate, and proficient. Due to the long duration of the videos, comprehension was required for long videos, which were divided equally into 2 to 4 equal parts and eventually compressed into 10-second segments for processing and analysis.

AVOS Annotated Videos of Open Surgery (AVOS) collected 1997 open surgery videos from YouTube, expanding 23 surgical procedure types and 50 countries over the last 15 years. Among them, 326³ videos are annotated with the action of the scene every five seconds. We first download the data from the dataset's homepage (<https://research.bidmc.org/surgical-informatics/avos>) and split the annotated videos to 5-second short clips, retaining the original frame rates and resolutions, with five action labels (cutting, suturing, typing, abstain and background). Finally, 27,745 clips with a total of 38.53 hours and 3,582,276 frames are obtained. The videos exhibit variable frame rates due to its multi-source nature, with the predominant FPS distribution concentrated within the range of 25 to 30.

³30 video urls have expired, so we only have 296 annotated videos